International Journal of Electrical, Electronic and Communication Sciences
ISSN: 2517-9438
Vol:2, No:10, 2008

Fuel Economy and Stability Enhancement of the Hybrid Vehicles by Using Electrical Machines on Non-Driven Wheels

P. Naderi, S.M.T. Bathaee, R. Hoseinnezhad and, R. Chini

***Abstract*—**Using electrical machine in conventional vehicles, also called hybrid vehicles, has become a promising control scheme that enables some manners for fuel economy and driver assist for better stability. In this paper, vehicle stability control, fuel economy and Driving/Regeneration braking for a 4WD hybrid vehicle is investigated by using an electrical machine on each non-driven wheels. In front wheels driven vehicles, fuel economy and regenerative braking can be obtained by summing torques applied on rear wheels. On the other hand, unequal torques applied to rear wheels provides enhanced safety and path correction in steering. In this paper, a model with fourteen degrees of freedom is considered for vehicle body, tires and, suspension systems. Thereafter, power-train subsystems are modeled. Considering an electrical machine on each rear wheel, a fuzzy controller is designed for each driving, braking, and stability conditions. Another fuzzy controller recognizes the vehicle requirements between the driving/regeneration and stability modes. Intelligent vehicle control to multi objective operation and forward simulation are the paper advantages. For reaching to these aims, power management control and yaw moment control will be done by three fuzzy controllers. Also, the above mentioned goals are weighted by another fuzzy sub-controller base on vehicle dynamic**.** Finally, Simulations performed in MATLAB/SIMULINK environment show that the proposed structure can enhance the vehicle performance in different modes effectively.

***Keywords*—**Hybrid, Pitch, Roll, Regeneration, Yaw

I. Introduction

ONE of the significant qualitative factors of the vehicle behavior is its stability in critical driving conditions such as braking on μ-Split road and rotation with high speed. Recent research results of fuel economy in the vehicles have led to invention of hybrid vehicles. In these vehicles, the driver power demand is provided by gasoline engine and electrical machine. In most researches, the goal of the control strategy is only based on the fuel economy. In [1], a model based on the real time road control strategy for parallel hybrid vehicles has been offered. An optimal control strategy that chooses the power split between the engine and electrical machine has been presented in [2] to minimize fuel consumption in parallel hybrid vehicles. In [3], fuel economy has been improved by using field oriented control of a permanent magnet motor and its belt coupling with crankshaft. A simulation program to simulate behavior of various components of hybrid vehicles has been exhibited in [4]. Some researchers have focused on the vehicles' stability. A driver-assist stability system and stability enhancement for all-wheel-drive electric vehicles has been introduced in [5-7]. This system has been proposed in [8] for two-motor-drive electric vehicle to enhance safety using a fuzzy logic based controller. In [9], by using an electrical machine on front and rear axles, stability enhancement and regenerative braking have been provided. Direct yaw rate control with road condition estimation and anti slip control have been proposed in [10]. In [11], for an electrical vehicle, a new estimation method of slip-rate has been presented. . In [12] by different vehicle parameters identifying and using the sliding mode control, the stability enhancement has been exhibited and in [13] a multi-objective robust parameter space steering controller for yaw stability improvement has been presented. Attentive to latest researches on vehicles, it seen there are not attention to improve of the fuel consumption, regenerative braking and stability enhancement in twin for the hybrid vehicles. Intelligent control to perform the power managing and yaw moment control base on the vehicle dynamical behavior and forward drive simulation are the paper advantages.

I. PROPOSED STRUCTURE

In the front differential vehicle, engine torque is applied to front axle. By using two electrical machines on rear wheels, the stability of vehicle in critical conditions drive and fuel consumption, will be improved. The unequal torques applied to rear wheels will bring vehicle dynamic control to path correction. On the other hand, summation of torques is an essential factor in power managing among engine and electrical machines. In fact, using electrical machines on non-driven wheels provides Driving/Regeneration and driver assist systems in braking and rotation for this kind of hybrid vehicle. Figure 1, shows controller structure and its Inputs/Outputs signals.

Peyman.Naderi is Academic member of Electrical Engineering Department, Islamic Azad University, Iran, Borujerd from 2002, (e-mail: Naderi@ee.kntu.ac.ir).

Seyed.Mohammad.Taghi.Bathaee is Academic member of Electrical Engineering Department, University of K.N.Toosi, Tehran, Iran, (e-mail: Bathaee@kntu.ac.ir).

Reza.Hoseinnezhad, is Research Fellow with the Department of Electrical & Electronic Engineering, Melbourne School of Engineering, the University of Melbourne. (e-mail: rezah@unimelb.edu.au)

Reza. Chini is member of Iranian Society of Mechanical Engineers since 2006., (e-mail: rezachini@gmail.com).

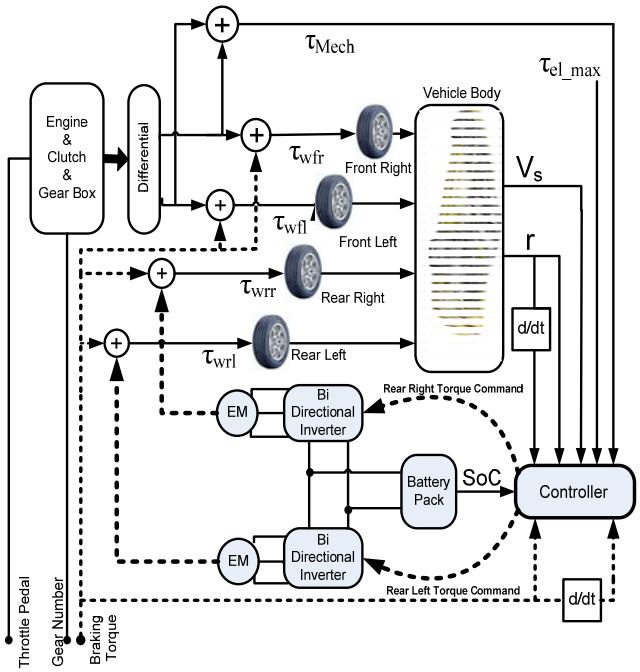

Fig. 1. Vehicle and controller structure

Definition of Controller Signals

Symbol	Definition
τ_{Mech}	Mechanical torque applied to driven wheels
τ_{el_max}	Maximum torque available from electrical machines
V_s	Vehicle speed
r	Vehicle yaw rate
SoC	Battery state of charge
τ_{wrl}	Torque applied to rear left wheel
τ_{wrr}	Torque applied to rear right wheel
τ_{wfl}	Torque applied to front left wheel
τ_{wfr}	Torque applied to front right wheel

II. VEHIVCLE MODELING

A model with fourteen degrees of freedom is used for simulation. In this model, the system dynamic can be described as follows. Six degrees are devoted to the chassis motion and eight degrees are assigned to wheels angular speed and wheels vertical movements [6].

A. Vehicle Body Modeling

Figure 2 and figure 3, shows different coordinates that are used for the modeling purpose.

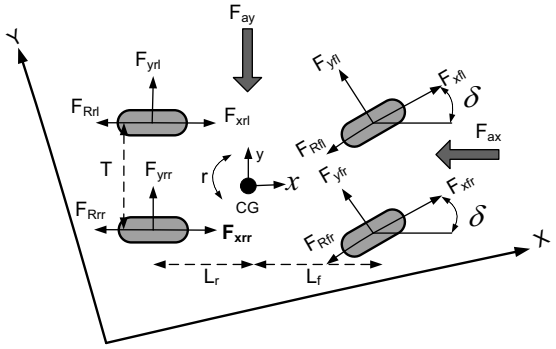

Fig. 2. Vehicle Body Model

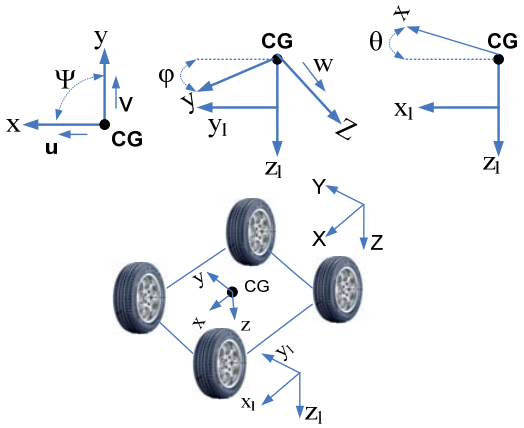

Fig. 3. Coordinated system for vehicle body model

Definition of Body Model Parameters

Symbol	Definition
δ	Steering angle
F_{xfl}	Longitudinal force of front left wheel
F_{xfr}	Longitudinal force of front Right wheel
F_{xrl}	Longitudinal force of rear left wheel
F_{xrr}	Longitudinal force of rear right wheel
F_{yfl}	Lateral force of front left wheel
F_{yfr}	Lateral force of front right wheel
F_{yrl}	Lateral force of rear left wheel
F_{yrr}	Lateral force of rear right wheel
F_{Rfl}	Rolling resistance of left front wheel
F_{Rfr}	Rolling resistance of right front wheel
F_{Rrl}	Rolling resistance of left rear wheel
F_{Rrr}	Rolling resistance of right rear wheel
CG	Corresponding to Centre of gravity of vehicle
X,Y	Denotation of static reference frame
x,y	Denotation of moving reference frame
T	Long of vehicle axle
L_f	CG distance from front axle
L_r	CG distance from rear axle
F_{ax}	Longitudinal aerodynamic drag force
F_{ay}	Lateral aerodynamic drag force

The moving parameters that are just six degree of freedom in the vehicle are illustrated as below table.

Six degrees of Freedom in Vehicle Center of Gravity

Symbol	Definition
u	Longitudinal velocity of CG
v	Lateral velocity of CG
w	Vertical velocity of CG
ψ	Yaw angle of CG
φ	Roll angle of CG
Θ	Pitch angle of CG

And definition of angular velocities of yaw, roll and pitch, can be followed as $r=\dot{\psi}$, $p=\dot{\varphi}$, $q=\dot{\Theta}$

B. Suspension Modeling

Quarter-vehicle model is used for each wheel. A model of the suspension system is shown in figure 4. Each wheel has an individual mass which is connected to the ground via the wheel virtual spring and damping and to the chassis via a spring-damping system [14].

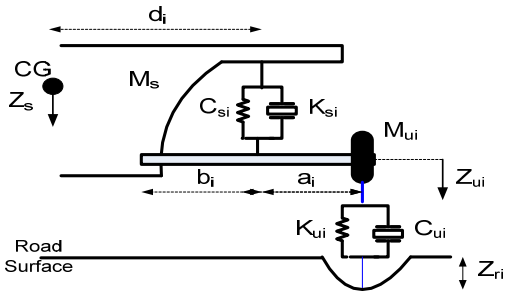

Fig. 4. Suspension system model

Suspension and Non-Sprung Mass Parameters

Symbol	Definition
K_{si}	Stiffness of suspension spring
C_{si}	Damping coefficient of suspension spring
K_{ui}	Stiffness factor of tire
C_{ui}	Damping factor of tire
M_{ui}	Unsprung mass weight
M_s	Sprung mass weight
Z_s	Height of sprung mass CG
Z_{ui}	Height of unsprung mass
Z_{ri}	Road roughness

C. Dynamic Equations

Considering the action forces on the vehicle, as depicted in figure 2, one can write the vehicle motion equation as below:

$$M_t(\dot{u}+qwrv) = M_s h(\dot{q}+pr)+F_{xfl}\cos(\delta)+F_{yfl}\sin(\delta)+ F_{xfr}\cos(\delta)+F_{yfr}\sin(\delta)+F_{xrl}+F_{xrr}-F_{ax} \quad (1)$$

$$M_t(\dot{v}+ru-pw) = M_s h(\dot{p}+qr)+F_{xfl}\sin(\delta)+F_{yfl}\cos(\delta)+ F_{xfr}\sin(\delta)+F_{yfr}\cos(\delta)+F_{yrl}+F_{yrr}-F_{ay} \quad (2)$$

$$I_z\dot{r} = (I_x I_y)pq+L_f[F_{xfl}\sin(\delta)+F_{yfl}\cos(\delta)+F_{xfr}\sin(\delta)+F_{yfr}\cos(\delta)]- L_r(F_{yrl}+F_{yrr})+T/2[F_{xfl}\cos(\delta)-F_{yfl}\sin(\delta)- F_{xfr}\cos(\delta)+F_{yfr}\sin(\delta)+F_{xrl}-F_{xrr}]+M_{zfl}+M_{zfr}+M_{zrl}+M_{zrr} \quad (3)$$

Where I_z, is the vehicle moment of inertia around the vertical exis and M_t, is total mass of vehicle. The vehicle roll motion satisfies the following equation:

$$I_{xs}\dot{p}+(I_{zs}-I_{ys})qr = \sum R_i.F_{si}+M_s g h\varphi-M_s h\,(\dot{v}+ru-pw) \quad (4)$$

Other Parameters of Sprung Mass

Symbol	Definition
I_{xs}	Vehicle sprung mass moment of inertia around x axis
I_{ys}	Vehicle sprung mass moment of inertia around y axis
I_{zs}	Vehicle sprung mass moment of inertia around z axis
R_1	$-d_1+(d_1-b_1)\,a_1/(a_1+b_1)$
R_2	$d_2-(d_2-b_2)\,a_2/(a_2+b_2)$
R_3	$-d_3+(d_3-b_3)\,a_3/(a_3+b_3)$
R_4	$d_4-(d_4-b_4)\,a_4/(a_4+b_4)$

Acting force on suspension system for each wheel can be carried out as:

$$F_{s1}=K_{s1}(z_{u1}-z_s+L_f\sin(\theta)+d_1\sin(\varphi))+ C_{s1}(w_{u1}-w+L_f q\cos(\theta)+d_1 p\cos(\varphi)) \quad (1\text{-}5)$$

$$F_{s2}=K_{s2}(z_{u2}-z_s+L_f\sin(\theta)-d_2\sin(\varphi))+ C_{s2}(w_{u2}-w+L_f q\cos(\theta)-d_2 p\cos(\varphi)) \quad (2\text{-}5)$$

$$F_{s3}=K_{s3}(z_{u3}-z_s-L_r\sin(\theta)+d_3\sin(\varphi))+ C_{s3}(w_{u3}-w-L_r q\cos(\theta)+d_3 p\cos(\varphi)) \quad (3\text{-}5)$$

$$F_{s4}=K_{s4}(z_{u4}-z_s-L_r\sin(\theta)-d_4\sin(\varphi))+ C_{s4}(w_{u4}-w-L_r q\cos(\theta)+d_4 p\cos(\varphi)) \quad (4\text{-}5)$$

Where w_{ui} is the vertical speed of the i^{th} wheel. Now the pitch rate can be carried out as in below:

$$I_{ys}\dot{q}+(I_{xs}-I_{zs})pr = -L_f(F_{s1}/R_{r1}+F_{s2}/R_{r2})+L_r(F_{s3}/R_{r3}+F_{s4}/R_{r4})+ h_{cg}[F_{xfl}\cos(\delta)-F_{yfl}\sin(\delta)+F_{xfr}\cos(\delta)-F_{yfr}\sin(\delta)+F_{xrl}+F_{xrr}] \quad (6)$$

Where:

Other Used Parameters in the Pitch Equation

Symbol	Definition
h_{cg}	Height of the CG
R_{ri}	$(a_i+b_i)/b_i$

Motion equation for the sprung mass in the vertical direction can be written as follows:

$$M_s(\dot{w}+pv-qu)=\sum(F_{si}/R_{ri}) \quad (7)$$

And the vertical movement of each unsprung mass is expressed by the following equation:

$$M_{ui}\dot{w}_{ui}=K_{ui}(z_{ri}-z_{ui})+C_{ui}(\dot{z}_{ri}-\dot{z}_{ui})-(F_{si}/R_{ri}) \quad (8)$$

C. Tire Modeling

Tire Modeling is one of the most important and ambiguous parts of vehicle modeling. Well known Dugoff's model for longitudinal and lateral forces has been used in this article [14].

$$\mu_i = \mu_{peak-i}(1 - A_s R_w\sqrt{\lambda_i^2 + Tan^2(\alpha_i)}) \quad (1\text{-}9)$$

$$H_i = \sqrt{\left[\left(\frac{C_x\lambda_i}{\mu_i F_{zi}(1-\lambda_i)}\right)^2 + \left(\frac{C_y Tan(\alpha_i)}{\mu_i F_{zi}(1-\lambda_i)}\right)^2\right]} \quad (2\text{-}9)$$

$$F_{xi} = \begin{cases} \frac{C_x\lambda_i}{1-\lambda_i} & \text{for} \quad H_i < 0.5 \\ \frac{C_x\lambda_i}{1-\lambda_i}\left(\frac{1}{H_i^2} - \frac{1}{4H_i^2}\right) & \text{for} \quad H_i \geq 0.5 \end{cases} \quad (3\text{-}9)$$

$$F_{yi} = \begin{cases} \frac{C_y Tan(\alpha_i)}{1-\lambda_i} & \text{for} \quad H_i < 0.5 \\ \frac{C_y Tan(\alpha_i)}{1-\lambda_i}\left(\frac{1}{H_i^2} - \frac{1}{4H_i^2}\right) & \text{for} \quad H_i \geq 0.5 \end{cases} \quad (4\text{-}9)$$

F_z is the vertical force on the tire considering effects of vehicle longitudinal and lateral accelerations and can be obtained as below.

$$F_{zfl}=M_t/(L_r+L_f).[g.L_r/2-a_x h_{cg}/2+a_y.L_r.h_{cg}/T] \quad (5\text{-}9)$$

$$F_{zfr}=M_t/(L_r+L_f).[g.L_r/2-a_x h_{cg}/2-a_y.L_r.h_{cg}/T] \quad (6\text{-}9)$$

$$F_{zrl}=M_t/(L_r+L_f).[g.L_f/2+a_x h_{cg}/2+a_y.L_f.h_{cg}/T] \quad (7\text{-}9)$$

$$F_{zrr}=M_t/(L_r+L_f).[g.L_f/2-a_x h_{cg}/2-a_y.L_f.h_{cg}/T] \quad (8\text{-}9)$$

Tire Parameters Definition

Symbol	Definition
λ	Wheel's slip
α	Wheel's slip angle
a_x	Longitudinal vehicle acceleration
a_y	Lateral vehicle acceleration
μ_i	Friction coefficient for i^{th} wheel
C_x	Longitudinal stiffness of tire
C_y	Lateral stiffness of tire

The speed vector of wheels can be written as:

$$V_{wfl} = (u - T/2\ r)\ i + (v + L_f\ r)\ j \quad (1\text{-}10)$$

$$V_{wfr} = (u + T/2\ r)\ i + (v + L_f\ r)\ j \quad (2\text{-}10)$$

$$V_{wrl} = (u - T/2\ r)\ i + (v - L_r\ r)\ j \quad (3\text{-}10)$$

$$V_{wrr} = (u + T/2\ r)\ i + (v - L_r\ r)\ j \quad (4\text{-}10)$$

Slip angle of wheels can be obtained as:

$$\alpha_{fl}=\delta - tg\text{-}1[(v+L_f\ r)/(u - T/2\ r)] \quad (1\text{-}11)$$

$$\alpha_{fr}=\delta - tg\text{-}1[(v+L_f\ r)/(u + T/2\ r)] \quad (2\text{-}11)$$

$$\alpha_{rl}= -tg\text{-}1[(v-L_r\ r)/(u - T/2\ r)] \quad (3\text{-}11)$$

$$\alpha_{rr}= -tg\text{-}1[(v-L_r\ r)/(u + T/2\ r)] \quad (4\text{-}11)$$

The slip of the wheels, for i: fl, fr, rl, rr can be written as:

$$\lambda_i = \begin{cases} 1 - \frac{R_w\omega_i}{|V_{wi}|Cos(\alpha_i)} & \text{for} \quad R_w\omega_i < |V_{wi}|Cos(\alpha_i) \\ -1 + \frac{R_w\omega_i}{|V_{wi}|Cos(\alpha_i)} & \text{for} \quad R_w\omega_i \geq |V_{wi}|Cos(\alpha_i) \end{cases} \quad (12)$$

Applying mover torque (τ_w) on the wheel, the rotation can be described as follows:

$$I_{wi}\ \dot{\omega_i} = \tau_{wi} - R_w F_{xi} - \tau_{Ri} - R_w F_{zi}.Sin(\beta) \quad (13)$$

Used Parameters in Wheel Rotation Equations

Symbol	Definition
ω	Wheel's angular speed
I_w	Wheel's moment of inertia
R_w	Wheel's radius
$\tau_R = C_0.F_z + C_1.\|V_w\|^2$	Wheel's rolling resistant torque
β	Road gradient

Usually, $0.04<C_0<0.02$ and $C_1<<C_0$. Now two degrees of freedom for each wheel are obtained which are consist of ω, w_u

III. POWERTRAIN MODELING

Transmission subsystem includes engine, gear box, clutch, brake, and differential. The output engine power is transferred to driven wheels via the clutch, gear box, and differential. Braking torque is transferred to all wheels directly by the brake pedal command. On account of the equality between input and output power in gear box and differential systems, modeling of these subsystems can be performed by assuming a constant coefficient for each of them. Engine and gear box speed equivalency is assumed for simulation purposes. Since this regulation would be violated in some cases such as low speed motion or driving by improper gear, the engine power will be wasted in clutch subsystem. Figure 6 shows transmission modeling. Figure 7 shows the clutch power transmission curve which is utilized in this work for simulation. The clutch is simulated by two surfaces. One of them is connected to engine shaft and the other one is jointed to gear box input.

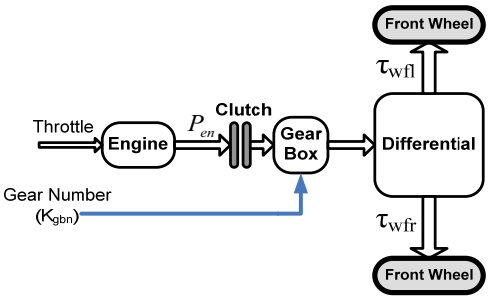

Fig. 5. Mechanical powertrain subsystems

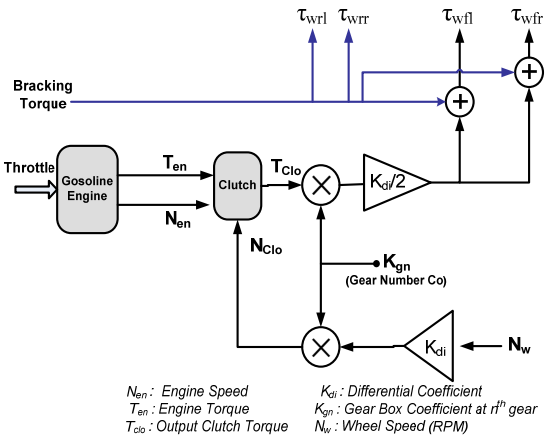

Fig. 6. Mechanical powertrain modeling

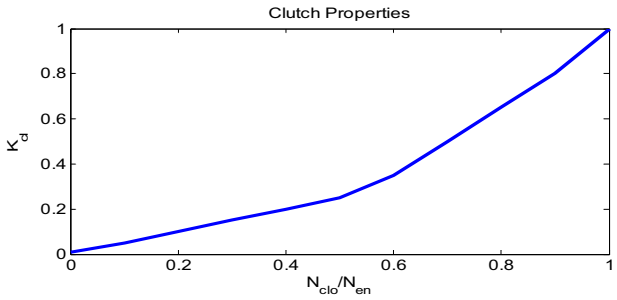

Fig. 7. Clutch curve model

Transmition Model Parameters

Symbol	Definition
K_{gn}	The n^{th} gear coefficient
K_{di}	Differential gear coefficient
N_{en}	Engine shaft speed
T_{en}	Engine output torque
N_{clo}	Gear box speed at the n^{th} gear speed
T_{clo}	Output torque of gear box at the n^{th} gear
$K_{cl}=T_{clo}/T_{cli}$	Clutch transferred torque coefficient

Engine torque and fuel consumption will be computed regarding to engine maps for modeling purposes. One of these maps computes the shaft torque based on throttle opening and shaft speed. The engine fuel consumption is determined according to shaft speed and shaft torque [15]. Sample maps are shows as figures 8 and 9.

IV. Electrical Devices

Electrical subsystems, used in this article, consist of AC/DC converter, electrical machine, batteries, and power electronic components. Because of fast dynamic of these subsystems in comparison with vehicle dynamic, only the battery's dynamical model is taken into account. In this way, the 'ADVISOR' statistical model has been used for Inverter/Electrical machine modeling [15-16]. Models demonstrated above were utilized in simulation part.

A. Electrical Machine Modeling

In electrical machine and connected inverter models, efficiency and maximum rotor torque are available. Figure 10 shows Inverter/Electrical machine maps as a sample.

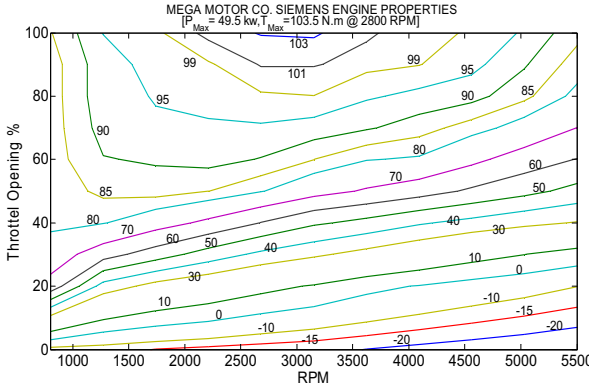

Fig. 8. The sample engine torque map

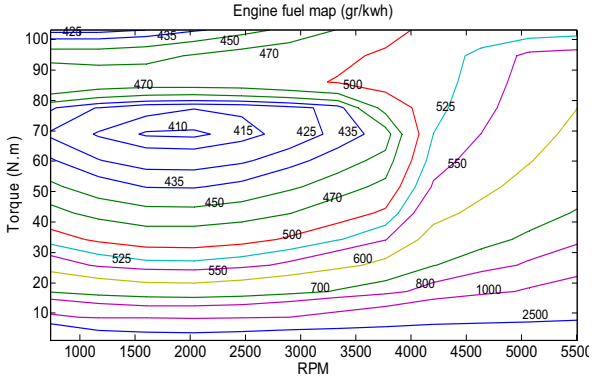

Fig. 9. The sample engine fuel map

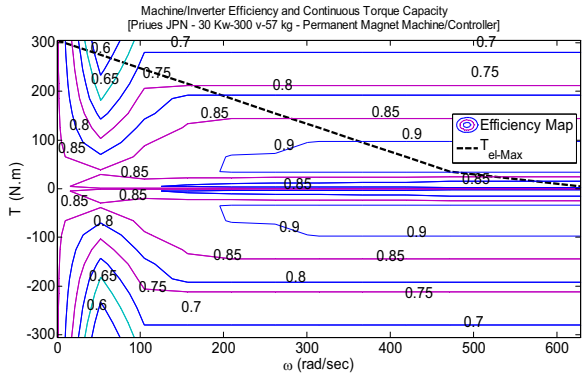

Fig. 10. Electrical machine curves

B. Battery Modeling

Battery state of charge (SoC) is the most important control signal in the hybrid vehicle. In this paper, one of the well known battery model has been employed. This model is based

on variable voltage source and internal variable resistance depending on SoC. Figures 11 and 12 show this model and typical values of its parameters. One of the simple and well known formulas for SoC calculation is given as below [16].

$$\mathrm{SoC} = \frac{(\mathrm{Ah_{cap}} - \mathrm{Ah_{used}})}{\mathrm{Ah_{cap}}} \quad (1\text{-}14)$$

$$\mathrm{Ah_{used}} = \mathrm{Ah_{cap}}(1 - \mathrm{SoC_{(0)}}) + \int_0^t \frac{\mathrm{I_b}}{3600}\,\mathrm{dt} \quad (2\text{-}14)$$

$$I_b = \frac{V_{oc} - \sqrt{4R_{int} - P_b}}{2R_{int}} \quad (3\text{-}14)$$

Where P_b is the battery power and:

Battery Model Parameters

Symbol	Definition
Ah_{cap}	Maximum Amper.hour capacity
$SoC_{(0)}$	Initial state of charge
I_b	Battery current

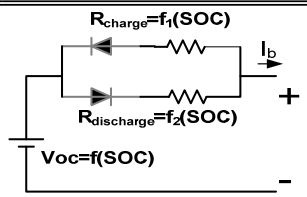

Fig. 11. R_Internal Battery Model

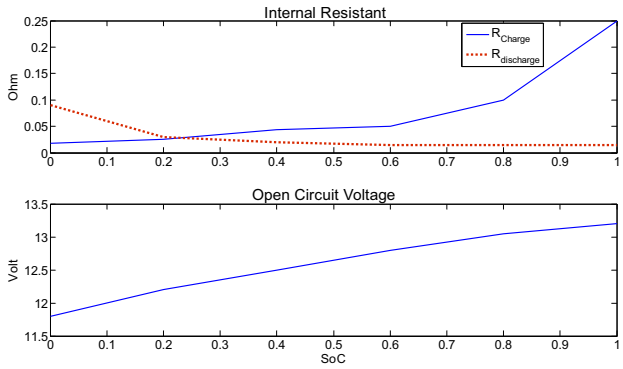

Fig. 12. Sample Battery Parameters

V. Driver Actions Modeling

A simple PID controller has been used for driver behavior simulation in Throttle/Brake pedals' pressure. In addition, for gear changing simulation, it is assumed that the changing is established upon throttle opening and vehicle speed experimental data.

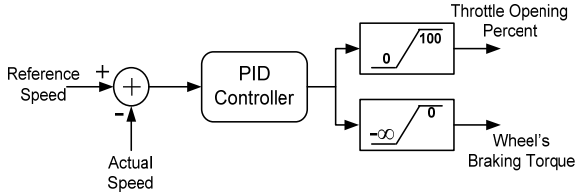

Fig. 13. Simple PID Controller for pedals pressure simulation

VI. Control Strategy

Regarding to (3), the yaw rate can be directly controlled by applying a differential input torque on non-driven wheels (F_{xrl}-F_{xrr}). From the steady state cornering theory of bicycle model, it is known that the yaw velocity of vehicle and yaw rate error satisfy the following equations [6].

$$\mathrm{r_d} = \left(\frac{\mathrm{V_s}}{\mathrm{L_f} + \mathrm{L_r}}\right).\delta \quad (15)$$

$$\mathrm{e_r} = \mathrm{r_d} - \mathrm{r} \quad (16)$$

Moreover, Driving/Regeneration braking can be obtained by summing torques applied on rear wheels which are called assistant forces (F_{xrl}+F_{xrr}). Controller structure and its input/output signals are shown in the figures 14. The controller will be performed the power management and yaw moment control in twin, controller is consisting of four sub-controllers to achievement of this purpose

A. Drive Mode

This mode will be activated in driving condition which driver power demand is positive. Electrical machine torques applied on rear wheels will be based on the mechanical torque applied to front wheels. If the mechanical torque applied be positive, electrical assisting torque will be produced. In this mode the maximum torque available of each electrical machine will be limited by a fuzzy controller. Also, applied torque by electrical machines, will be controlled base on SoC and vehicle speed by this controller.

B. Grad Mode

Base on the figure 8, in same case the engine torque is negative (such as throttle opening=0% in all engine speeds). This case is occur in same case such as motion in grad and may be not any pressure on brake pedal. In this condition electrical machines operation will be changed to generation mode for regenerative operation.

C. Brake Mode.

This mode will be activated by brake pedal pressured. In this case electrical torque applied will be negative to performed regenerative braking and generation mode operation of electrical machines to battery charging. Torque applied by electrical machine will be controlled by a fuzzy controller base on the brake pedal pressure condition.

D. Stability Mode

In three previous modes, sum of the torques applied to rear wheels will be determined. But, stability sub-controller will be computed the different torques of electrical machines based on the bicycle theory.

E. Goal Management

The Driving/Regenerative torque applied by electrical machines may be near to maximum torque capacity of electrical machine. In this case, if the yaw rate error exists, applying the computed torque by the stability mode sub-controller will be impossible. In order to solve this problem, base on vehicle dynamic, the above mentioned goals are

weighted by goal managing sub-controller. Figure 14 shows the overall controller. As shown in this figure, the engine torque is one of the input signals. Due to difficulty its measurement, this quantity can be obtained from the engine map such as figure 8.

Overall controller Parameters

Symbol	Definition
τ_{el_max}	Maximum torque available of electrical machine
SoC	Battery state of charge
V_s	Normalized vehicle speed
τ_{en}	Engine torque
X_{bp}	Normalized brake pedal displacement
e_r	Yaw rate error compared with bicycle theory
K_{di}	Differential coefficient
K_{Gn}	Gear coefficient at n^{th} gear
τ_{Rotor}	Sum of torque applied to rear wheels
τ_{Rotor_l}	Rear left torque applied by electrical machine
τ_{Rotor_r}	Rear right torque applied by electrical machine
$\Delta\tau_{Rotor}$	Different of electrical machines torque
K_a	Drive assist fuzzy controller output
K_r	Braking fuzzy controller output
K_d	Stability fuzzy controller output
K_m	Goal managing fuzzy controller output
τ_{Com}	Torque command for Driving/Regenerative

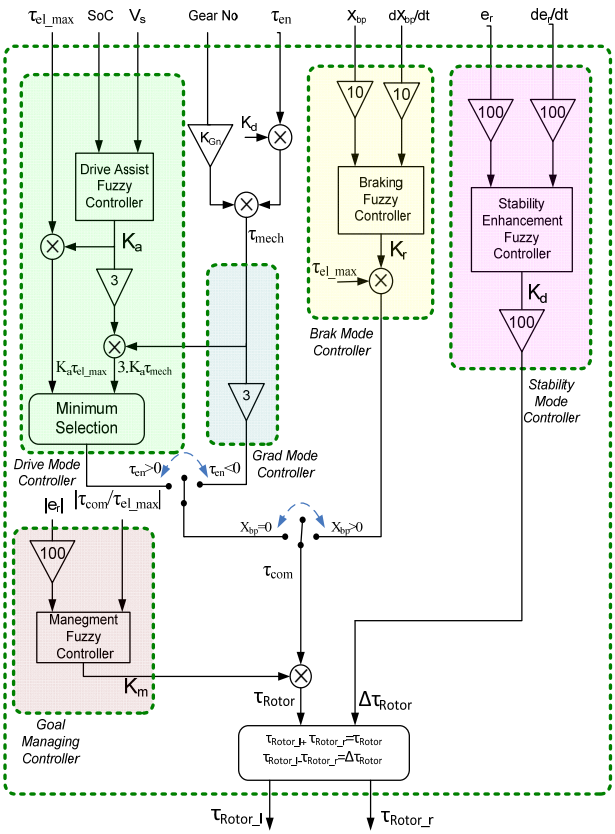

Fig. 14. Proposed controller

According to figure 14 and regarding to *A-E* subsections, The controller aims can be summarized as below:

- *If the engine torque be positive, assistant power applied by electrical machines, be about threefold of engine power in best condition (Best SoC and low speed)*
- *If the engine torque be negative and there is no pressure on brake pedal, regenerative power applied by electrical machines, be threefold of engine power in all condition (there is no relation between SoC and vehicle speed or etc).*
- *By braking pedal pressure, regenerative power applied by electrical machines, be relative to braking pedal displacement and its rapidity.*
- *Yaw moment control, be active in all conditions.*
- *Due to electrical machines torque limitation, torque saturation may be occur by Driving/Regeneration torque applied. In this case, Driving/Regeneration torque applied will be decreased by a fuzzy controller before saturation to avoid of electrical machines torque saturation.*
- *If SoC be lower than specified value (0.6), assist torque applying will be stopped until reaching of the SoC to specified high value (0.8). This rule is assumed in simulation, but is not shown in figure 14.*

Fuzzy membership's functions, and rule bases are presented as following. These are adjusted by expert and experiential Knowledge. In the brake mode controller, for prohibition of shake occurrence during of braking, the input signals are bases on the brake pedal displacement and its intensity.

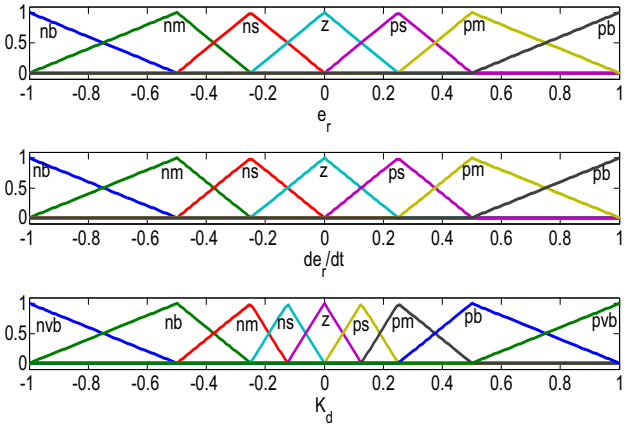

Fig 15. Stability fuzzy controller memberships

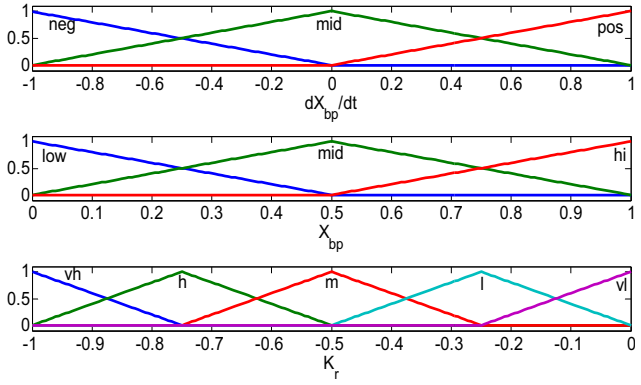

Fig. 16. Braking fuzzy controller memberships

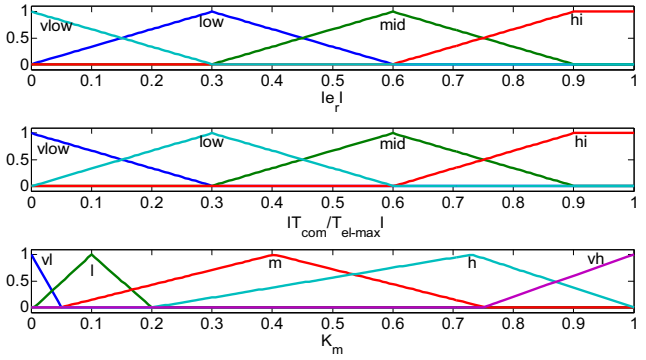

Fig. 17. Goals management controller memberships

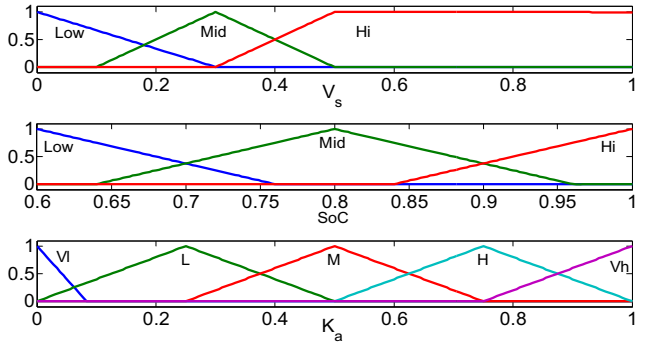

Fig. 18. Drive assists fuzzy controller memberships

TABLE I
STABILITY FUZZY CONTROLLER RULE BASE

STABILITY MODE		e_r						
		nb	nm	ns	z	ps	pm	pb
de_r/dt	nb	nvb	nvb	nvb	nb	nm	ns	z
	nm	nvb	nvb	nb	nm	ns	z	ps
	ns	nvb	nb	nm	ns	z	ps	pm
	z	nb	nm	ns	z	ps	pm	pb
	ps	nm	ns	z	ps	pm	pb	pvb
	pm	ns	z	ps	pm	pb	pvb	pvb
	pb	z	ps	pm	pb	pvb	pvb	pvb

TABLE II
DRIVE ASSIST CONTROLLER RULE BASE

DRIVE MODE		Vs		
		Low	Mid	Hi
SoC	Low	VL	VL	VL
	Mid	H	M	L
	Hi	VH	H	M

TABLE III
BRAKE MODE FUZZY CONTROLLER RULE BASE

BRAKE MODE		dX_{bp}/dt		
		pos	mid	neg
X_{bp}	hi	vh	h	m
	mid	h	m	l
	low	m	l	vl

TABLE IV
GOAL MANAGING FUZZY CONTROLLER RULE BASE

GOAL MANAGMENT		$\lvert\tau_{com}/\tau_{el\_max}\rvert$			
		vlow	low	mid	hi
$\lvert e_r \rvert$	vlow	vh	vh	vh	vh
	low	vh	vh	h	m
	mid	vh	h	m	l
	hi	vh	m	l	vl

VII. SIMULATION RESULTS

Certain parameters of an automobile named 'KIA' are tabulated as below for simulation:

TABLE V
ENGINE DATA

Parameter	Symbol	Unit	Value
Maximum Power	$P_{en}(max)$	Kw	50
Maximum Torque	$\tau_{en}(max)$	N.m	103.3
Maximum Speed	$\omega_{en}(max)$	RPM	5500

Engine Maps: Base on the figures 8 and 9

TABLE VI
. WHEEL DATA

Parameter	Symbol	Unit	Value
Longitudinal stiffness	C_x	N	17500
Lateral stiffness	C_y	N/rad	15000

TABLE VII
GEAR BOX DATA

Parameter	Symbol	Unit	Value
1	3.454	K_{g1}	1
2	1.944	K_{g2}	2
3	1.275	K_{g3}	3
4	0.861	K_{g4}	4

Gear Changing is based on throttle opening and vehicle speed

TABLE VIII
VEHICLE BODY AND SUSPENSION DATA

Parameter	Symbol	Unit	Value
Total Vehicle Mass	M_t	Kg	1160
Inertia Coefficient	I_x,I_{xs}	Kgm^2	347
Inertia Coefficient	I_y,I_{ys}	Kgm^2	1676
Inertia Coefficient	I_z,I_{zs}	Kgm^2	7809
Spring Constant of Front Springs	K_{sf}	N/m	15400
Spring Constant of Rear Springs	K_{sr}	N/m	19000
Coefficient of Front Dampers	C_{sf}	Ns/m	1150
Coefficient of Rear Dampers	C_{sr}	Ns/m	6000
Spring Constant of all Tiers	K_u	N/m	175000
Coefficient of Tier Dampers	C_u	Ns/m	50
Distance from Front Axle toCG	L_f	m	1.097
Distance from Rear Axle to CG	L_r	m	1.247
Track Width	T	m	1.4
Tiers Mass	M_u	Kg	34.5
Height of CG	h_{cg}	m	0.43
Suspension Dimension	a_i	m	0.1
Suspension Dimension	b_i	m	0.2
Suspension Dimension	d_1,d_2	m	0.997
Suspension Dimension	d_4,d_4	m	1.147
Drag Coefficient	C_d	$N.S^2/m^2$	0.41
Frontal Area	A_F	m^2	1.8
Lateral Area	A_L	m^2	4.5
Wheels Radius	R_w	m	0.272
Wheels Inertia	I_w	Kgm^2	3.264

TABLE IX
DIFFERENTIAL AND CLUTCH DATA

Parameter	Symbol	Unit
Differential coefficient	K_d	3.78

Clutch curve is according to figure 7

TABLE X
BATTERY DATA

Parameter	Symbol	Unit	Value
Capacity	A.h	18	Capacity
Number	No unit	25	Number
Total Weight	Kg	167	Total Weight

TABLE XI
ELECTRICAL MACHINE AND INVERTER DATA

Parameter	Symbol	Unit
Maximum Power	KW	30
Nominal Voltage	V	300
Weight	Kg	57

After installing electrical components which change the vehicle into hybrid one, some parameters will be differed as shown in Table XII.

TABLE XII
APPROXIMATELY CHANGED PARAMETERS

Parameter	Symbol	Unit	Value
Total Vehicle Mass	M_t	Kg	1460
Distance from Front Axle to CG	L_f	m	1.197
Distance from Rear Axle to CG	L_r	m	1.147
Rear Tiers Mass	M_{u3} , M_{u4}	Kg	95
Height of CG	h_{cg}	m	0.3
Suspension Dimension	d_1,d_2	m	1.097
Suspension Dimension	d_3,d_4	m	1.047

In the next step, some various scenarios will be simulated and the comparison will be done in order to evaluate the proposed structure performance.

A. Steering with Constant Speed

This simulation performs motion at 50 km/h and steering as shown in figure 19. Figure 20 shows the vehicle lane in conventional and hybrid case by compared with reference lane base on bicycle theory. Also, yaw rates and electrical applied torques are shows in figure 19 and 21 respectively. According to figure 20, the conventional vehicle is in under steering condition. The vehicle in hybrid case has better stability due to electrical machines torque applied to rear wheels. So, the yaw rate in hybrid case is very near to reference value.

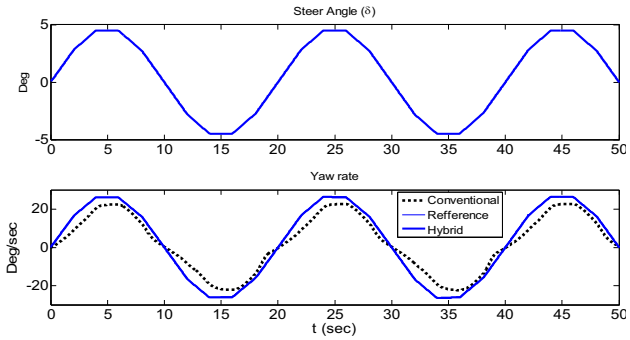

Fig 19. Steering angle and vehicle yaw rate

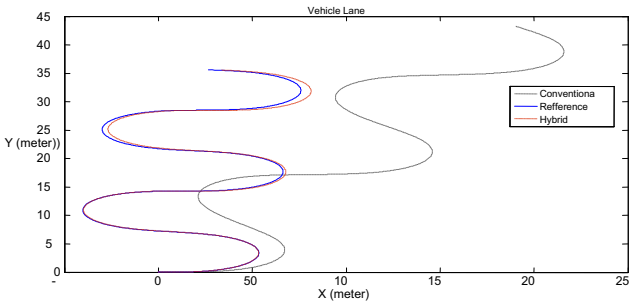

Fig. 20. Vehicle lane

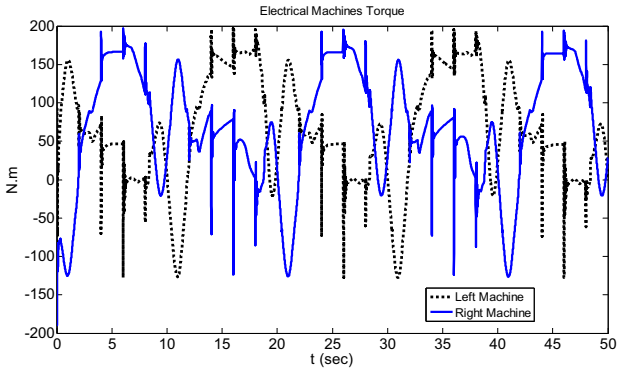

Fig. 21. Electrical machines torque

B. Braking on μ-Split Road

In this part braking at 110 km/h on a μ-split road (corresponding to dry pavement, μ=0.95, on the right side and unpacked snow, μ=0.35, on the left) has been simulated. During simulation, the steer angle is assumed to be zero. The vehicle speed reduction and simulation results are depicted in figure 22. This figure shows that the hybrid vehicle has better stability during braking and the undesired lane change is also lower than the conventional one.

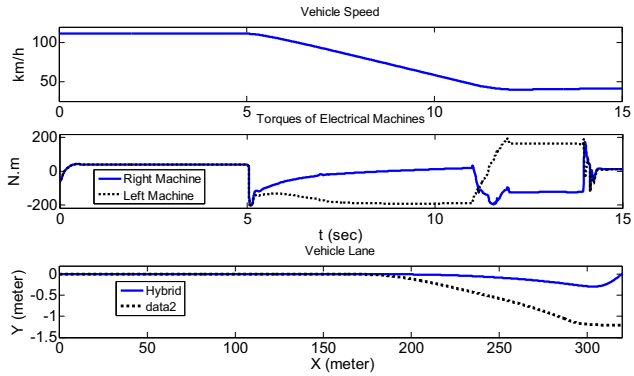

Fig. 22. Vehicle speed, electrical machines torque and vehicle lane during of braking

C. Motion on Steep Road and Regeneration Testing

Next simulation performs motion at 50 km/h on a steep road. Road gradient is shown in figure 23. During of simulation, the steering angle is assumed to be fixed at zero value and initial state of charge is assumed to 0.95. Engine and gear box behavior in conventional and hybrid case are compare in figure 25. Also electrical machines torque and battery state of charge are shows in figure 24. Lower part of figure 23 shows braking torque applied to each wheel in conventional and hybrid case.

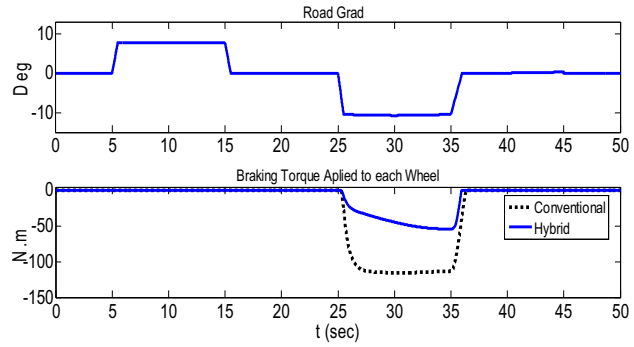

Fig. 23. Road gradient and braking applied torque

Regarding to figure 24, the battery will be charged during of braking. As seen in figure 23, the vehicle in hybrid case has lower enforced braking torque that is corresponding to regenerative braking condition. Also figure 25 shows lower engine output power in hybrid case compared to conventional one due to power management performed by controller.

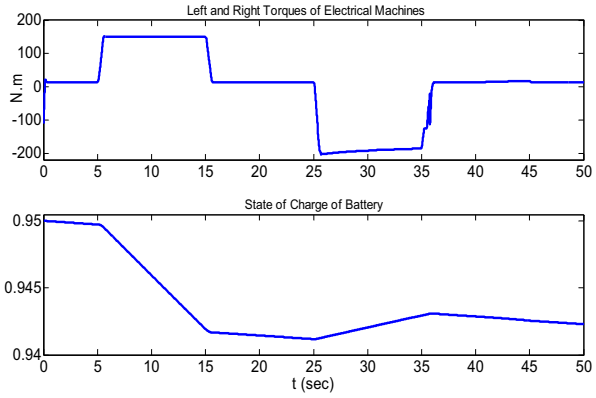

Fig. 24. Electrical machines torque and SoC

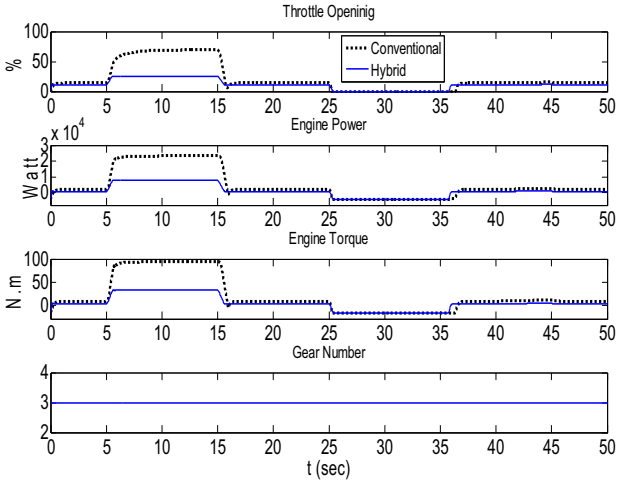

Fig. 25. Engine and gear box behavior

D. Civic Driving Cycle for Fuel Economy Testing

Three standard driving cycles which are shown in figure 26 are used for simulations [15]. Engine behavior, Battery operation, electrical machines torques, and braking torque for 'INDIA' driving cycle are shown in figures 27-29. Fuel consumptions for all of these three driving cycles are tabulated in Table XIII.

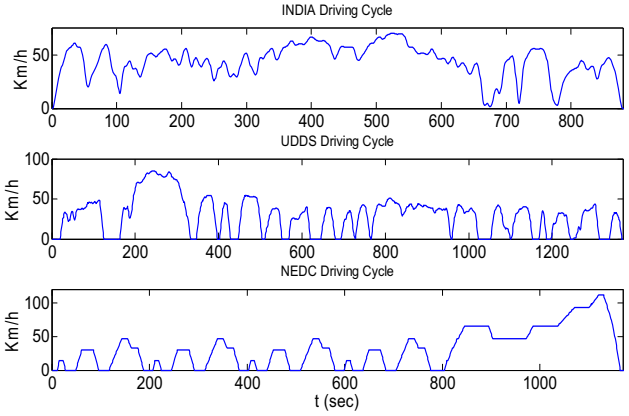

Fig. 26. Standard civic driving cycle

TABLE XIII
FUEL CONSUMPTION AND COMPARISON

CYCLE NAME	CONVENTIONAL LITER per 100 km	HYBRID LITER per 100 km	FUEL ECONOMY
INDIA	5.705	3.578	37.28%
UDDS	7.469	5.194	30.45%
NEDC	7.389	5.089	31.12%

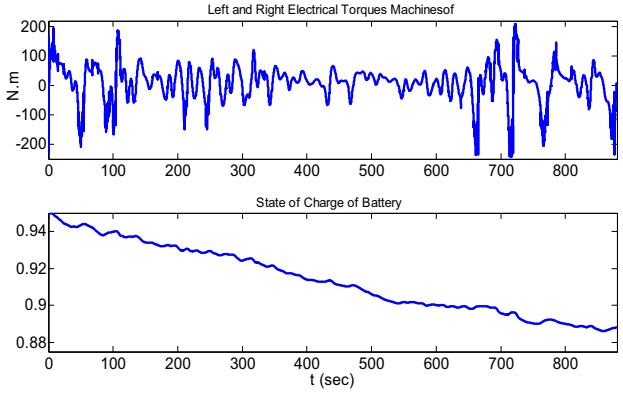

Fig. 27. Electrical machines torque and battery state of charge during INDIA driving cycle

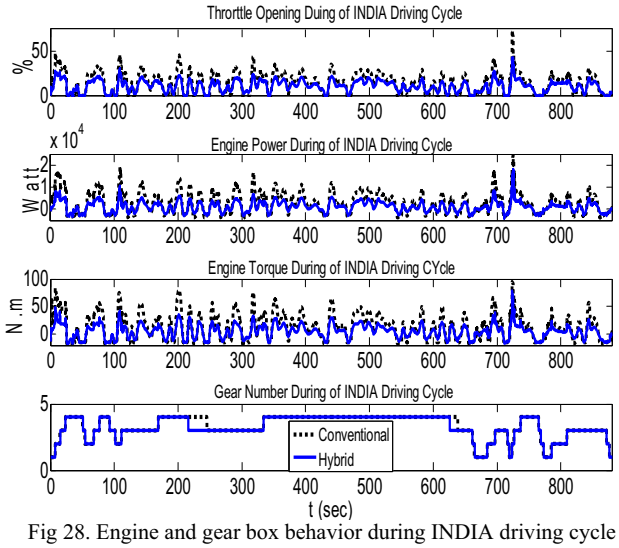

Fig 28. Engine and gear box behavior during INDIA driving cycle

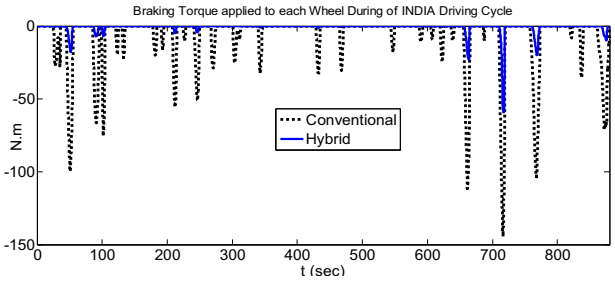

Fig. 29. Braking torque applied during of INDIA driving cycle

Electrical machines torques equality due to driving on direct lane is shown in figure 27. Regarding to figure 28, the engine output power in the hybrid case is lower than conventional one. Also figures 27 and 29 shows that the battery will be charged in the vehicle speed reduction and the braking torque applied will be decreased in the hybrid case. Table XIII, shows fuel economy obtained.

VIII. CONCLUSION

In this paper, a novel driver-assistant stability system and Driving/Regeneration braking for a front differential vehicle have been introduced by using electrical traction system on rear wheels. Fuzzy sub-controllers have been proposed for multi objective vehicle control to perform Driving/Regeneration and stability enhancement. The intelligent performance of the overall control system to make electrical machines torque commands base on the driving necessities and vehicle dynamical condition is the main advantage the proposed controller. Simulation results have shown intelligent performance of the proposed control system in various driving environments such as slippery road.

REFERENCES

[1] A.Sciarretta, M.Back, L.Guzzella, "Optimal Control of Parallel Hybrid Electric Vehicle", IEEE Transaction on control system Technology. Vol. 12. No. 3. May 2004
[2] S.Delpart, J.Lauber, T.Marie, J.Rimaux, "Control of a Parallel Hybrid Powertrain Optimal Control", IEEE Transaction on Vehicular Technology. Vol. 53. No. 3. May 2004
[3] R.I.Davis, R.D.Lorenz, " Engine Torque Ripple Cancellation with an Integrated Starter Alternator in a Hybrid Electric Vehicle: Implementation and Control" , IEEE conference, 2002, p. 2016-2021.
[4] J.V. Mierlo, P.V.D.Bossche, G.Maggetto, " Models of energy sources for EV and HEV:fuel cells, batteries ultracapacitors, flywheels and engine-generators" Elsevier, Jornal of power sources, 128, 2004,p. 76-89.
[5] F.Tahami, R.Kazemi, S.Farhangi, " A Novel Driver Assist Stability System for All Wheels drive Electric Vehicles", IEEE Transaction on Vehicular Technology, Vol. 52, No.3, May 2003.
[6] F.Tahami, R.Kazemi, S.Farhangi, " Fuzzy Based Stability Enhancement System for Four-Motor-Wheel Electric Vehicles". SAE 2002 Transactions.
[7] F.Tahami, R.Kazemi, S.Farhangi. " Direct Yaw Control of an All-Wheel-Drive EV Based on Fuzzy Logic and Neural Networks". 2003-01-0956 SAE World Congress.
[8] F.Tahami, R.Kazemi, S.Farhangi. " Stability Assist System for a two-Motor-Drive Electric Vehicle using Fuzzy Logic" 2003-01-1285 SAE World Congress.
[9] D.Kim, S.Hwang, H.Kim, " Rear Motor Control for 4WD Hybrid ElectricVehicle Stability", IEEE Conference, 2005, p. 86-91.
[10] H.Fujimoto, A.Tsumasaka, T.Noguchi, " Direct Yaw-moment Control of Electric Vehicle Based on Cornering Stiffness Estimation". IEEE conference, 2005. p. 2626-2631
[11] H.Fujimoto, K.Fujii, N.Takahashi, " Traction and Yaw-rate Control of Electric Vehicle with Slip-ratio and Cornering Stiffness Estimation". American Control Conference, july 2007. p. 5742-5747.
[12] M.Ouladisine, H.Shrain, L.FDridman, H.Noura, " Vehicle Parameters Estimation and Stability Enhancement using the Principle of Sliding Mode", American Control Conference, july 2007. p. 5224-5229.
[13] S.Oncu, S.Karaman, L.Guvence, " Robust Yaw Stability Controller Design for a Light Commercial Vehicle Using a Hardware in the Loop Steering Test Rig". IEEE Intelligent Vehicle Symposium, June 2007, p. 852-859.
[14] Weidong Xiang, Paul C. Richardson, Chenming Zhao, and Syed Mohammad, "Automobile Brake-by-Wire Control System Design and Analysis", IEEE Transaction on Vehicular Technology, Vol. 57, No.1, January 2008.
[15] ADVISOR Guide , Advisor, Vehicle simulation program
[16] Peyman.Naderi, Ali. Farhadi, S.M.Tahghi.Bathaee,"Forward Simulation of parallel hybrid vehicle and fuzzy controller design for Driving/Regeneration propose", pp,595-602, Waset Conference, Venice, October 2008, Vol.34.

Peyman Naderi received the B.Sc. degree in electronic engineering from Islamic Azad University of Iran, Dezful, in 1998 and M.S degree in power engineering from Chamran University, Iran, Ahvaz in 2001. He is currently PhD student in power engineering department of K.N.Toosi university, Iran, Tehran. From 2002 he is academic member of electrical engineering department of Islamic Azad university of Iran-Borujerd. His interests are hybrid vehicles, power system transient and power system dynamic.

S.M.Taghi Bathaee received his B. Sc., degree in power engineering from the K.N.Toosi University of Tehran, Iran and M. Sc and PhD degree in power engineering from Amir Kabir University of Tehran, Iran, in 1996. Hi is currently professor assistant in electrical engineering department of K.N.Toosi University of Tehran. His interests are electric and hybrid vehicles, power system transient, power system dynamic and control, power electronics and drive.

Reza Hoseinnezhad received his B.Sc., M.Sc. and Ph.D. degrees from the University of Tehran, Iran, in 1994, 1996 and 2002, respectively. Since 2002, he has held various academic positions at the University of Tehran, Swinburne University of Technology, Victoria, Australia, and The University of Melbourne, Victoria, Australia. He is currently a Research Fellow with the Department of Electrical & Electronic Engineering, Melbourne School of Engineering, The University of Melbourne.

Reza Chini received his B.S. in fluid mechanical engineering in 2005 and then in 2008, his M.S. in the subject of diagnostic system design for Diesel engines' air path from mechanical engineering department of K.N.Toosi university of Technology, Tehran, Iran. His research interests are vehicle dynamics, intelligent systems and fault diagnosis of nonlinear systems. Mr. Chini has been a member of Iranian Society of Mechanical Engineers since 2006.